AIP | Applied Physics Letters

Electrical limit of silver nanowire electrodes: Direct measurement of the nanowire junction resistance

Franz Selzer, Carlo Floresca, David Kneppe, Ludwig Bormann, Christoph Sachse, Nelli Weiß, Alexander Eychmüller, Aram Amassian, Lars Müller-Meskamp, and Karl Leo

Citation: Applied Physics Letters **108**, 163302 (2016); doi: 10.1063/1.4947285
View online: http://dx.doi.org/10.1063/1.4947285
View Table of Contents: http://scitation.aip.org/content/aip/journal/apl/108/16?ver=pdfcov
Published by the AIP Publishing

Electrical limit of silver nanowire electrodes: Direct measurement of the nanowire junction resistance

Franz Selzer,[1,a),b)] Carlo Floresca,[2] David Kneppe,[1,b)] Ludwig Bormann,[1,b)] Christoph Sachse,[1,b)] Nelli Weiß,[3] Alexander Eychmüller,[3] Aram Amassian,[4] Lars Müller-Meskamp,[1,b)] and Karl Leo[1,5]

[1]*Institut für Angewandte Photophysik (IAPP), Technische Universität Dresden, D-01062 Dresden, Germany*
[2]*NanoInstruments Division, DCG Systems, Richardson, Texas 75081, USA*
[3]*Physikalische Chemie, Technische Universität Dresden, D-01062 Dresden, Germany*
[4]*King Abdullah University of Science and Technology (KAUST), KSA-23955-6900 Thuwal, Saudi-Arabia*
[5]*Canadian Institute for Advanced Research (CIFAR), Toronto, Ontario CA-M5G 1Z8, Canada*

(Received 25 August 2015; accepted 11 April 2016; published online 19 April 2016)

We measure basic network parameters of silver nanowire (AgNW) networks commonly used as transparent conducting electrodes in organic optoelectronic devices. By means of four point probing with nanoprobes, the wire-to-wire junction resistance and the resistance of single nanowires are measured. The resistance R_{NW} of a single nanowire shows a value of $R_{NW} = (4.96 \pm 0.18)\,\Omega/\mu m$. The junction resistance R_J differs for annealed and non-annealed NW networks, exhibiting values of $R_J = (25.2 \pm 1.9)\,\Omega$ (annealed) and $R_J = (529 \pm 239)\,\Omega$ (non-annealed), respectively. Our simulation achieves a good agreement between the measured network parameters and the sheet resistance R_S of the entire network. Extrapolating R_J to zero, our study show that we are close to the electrical limit of the conductivity of our AgNW system: We obtain a possible R_S reduction by only ≈20% (common $R_S \approx 10\,\Omega/sq$). Therefore, we expect further performance improvements in AgNW systems mainly by increasing NW length or by utilizing novel network geometries. *Published by AIP Publishing.* [http://dx.doi.org/10.1063/1.4947285]

State-of-the-art metal nanowire networks (NWs) exhibit low sheet resistance R_S as well as high transmittance.[1] Therefore, these networks have been implemented as transparent conducting electrodes in various optoelectronic devices, in particular, in small molecule or polymer-based solar cells and light emitting diodes.[1–3] Currently, they allow the fabrication of flexible lab-scale devices showing performance parity with devices comprising the considerably more brittle and sputter-deposited indium tin oxide (ITO).[4]

Still, one important challenge is to further decrease the corresponding R_S of AgNW networks, since future products are expected to be fabricated on large area and curved substrates. Their size will clearly exceed the typical lab scale device which leads to much larger voltage drops and to a worse charge collection in the product if the sheet resistance cannot be decreased further. Consequently, these devices are expected to show an effectively poorer device performance in relation to their active area.[5,6]

Here, we evaluate a possible further sheet resistance reduction by determining the electrical limit of silver nanowire electrodes. As commonly known for percolation-based electrodes the sheet resistance is connected with the transmittance in such a way that a lower transmittance results in a lower sheet resistance, since more interconnections are established in the network.[14] In order to maintain high transmittance, the R_S of a nanowire network can only be reduced by reducing the basic network parameters, in particular, the resistance of the single nanowire R_{NW} and the wire-to-wire junction resistance R_J. The resistance of a nanowire is mainly influenced by the NW material and diameter, limiting a significant improvement in conductivity. Therefore, research efforts have focused mainly on reducing the initially high wire-to-wire resistances by several orders of magnitude, e.g., with heating, solvent washing, galvanic treatment, and plasmonic welding.[7–11] However, a detailed study on the basic network parameters has not been performed so far, leaving the question about the theoretical sheet resistance limit of silver nanowire electrodes open.

In this study, we measure the basic network parameters of a freshly prepared and an annealed network. After a thermal treatment, typically the sheet resistance is reduced by several orders of magnitude. Predominately, the insulating polymer shell around the wires gets softer and partially decomposes such that the wires can establish a larger contact area at the junctions.[12] This distinctly reduces the sheet resistance but does not significantly influence the transmittance. In a simulation, the measured network values R_{NW} and R_J are correlated with the R_S of the entire mesh. Consequently, we can extrapolate an electrical limit for our silver nanowire network by reducing the junction resistance to zero. Our investigations show that we are quite close to the electrical limit, since the measured R_J of our annealed AgNW network is almost negligible compared to the overall resistance.

All experiments were performed on cleaned BK7 glass substrates (Schott, Mainz, Germany) and pre-treated by oxygen plasma. Silver nanowires (AgNWs) SLV-NW-90 (Blue Nano, Charlotte (NC), USA) with a mean diameter of 90 nm and a mean length of 25 μm were obtained in ethanol. The

[a)]Electronic mail: franz.selzer@iapp.de
[b)]www.iapp.de

dispersions were diluted down to 0.2 mg/ml by adding ethanol and were spray-coated with a nozzle (Fisnar, Wayne (NJ), USA) onto a substrate with a temperature of 80 °C, guaranteeing a fast ethanol evaporation. The spraying distance, moving speed, and spraying pressure of the nozzle were 12 cm, 1.5 cm/s, and 200 mBar, respectively. Specular transmittance measurements were performed using a UV-VIS spectrometer (Shimadzu). The corresponding total transmittance (including substrate) was obtained by using an integrating sphere. A four point probe setup (Lucas Labs) was used for measuring the sheet resistance. After characterization, the as-sprayed AgNW samples were annealed at 210 °C for 90 min in air such that the nanowire geometry (length and diameter) was maintained and no significant change in transmittance was observed. A SEM (Carl Zeiss) was used for acquiring scanning electron microscopy images. Four point probing on silver nanowires was carried out with a nanoprobing system (dProber by DCG Systems). The nano-manipulated measurement tips consist of tungsten having a diameter of ≈50 nm. The tungsten tips were always cleaned before each measurement by contacting two tips and applying a distinct voltage for 1 min in order to remove native tungsten oxide from the tip surface. The corresponding current voltage data were obtained by measuring a sweep with an SMU (Keithley). Prior to the measurement, a junction or a single wire was electrically isolated from the network by gently scratching away the surrounding connections using the tungsten tips. The network simulation is divided into three parts: (1) generation of a randomly distributed network of lines on a 100 × 100 μm large area; (2) geometric calculation of intersections and assignment of corresponding resistance values into a knot list, both steps using a self-programmed routine in octave; and (3) the final evaluation of the knot list using the circuit simulation tool ngspice. As input, the average nanowire length and corresponding standard deviation according to the supplier's data sheet, the desired nanowire resistance R_{NW} and junction resistance R_J are used. The corresponding specular transmittance was controlled via the number of nanowires according to the surface coverage with 90 nm thick wires.

For measuring the resistance of single nanowires and isolated junctions, we use the setup illustrated in Fig. 1. By means of nano-manipulating tungsten tips (diameter ≈50 nm), installed inside a scanning electron microscope, a nanowire junction was isolated. Two of the six tungsten tips are exclusively used to carefully scratch and separate the nanowires, isolating them from neighboring wires. The remaining four tips are used to four point probe the junction resistance R_J of the isolated junction. Here, a current voltage sweep is carried out and the corresponding resistance is extracted from the linear slope. Furthermore, at least three different measurement positions are investigated to ensure a well established electrical connection between the measurement tips and the nanowires. Since nanoprobing directly at the junction may alter its properties and characteristics, we always contact the nanowires in a defined distance to the junction. Consequently, the junction resistance R_J needs to be extracted from the measured resistance given by $R_{meas} = R_{NW1} + R_{NW2} + R_J$. Therefore, we also perform measurements to obtain the resistance of a single nanowire R_{NW} with

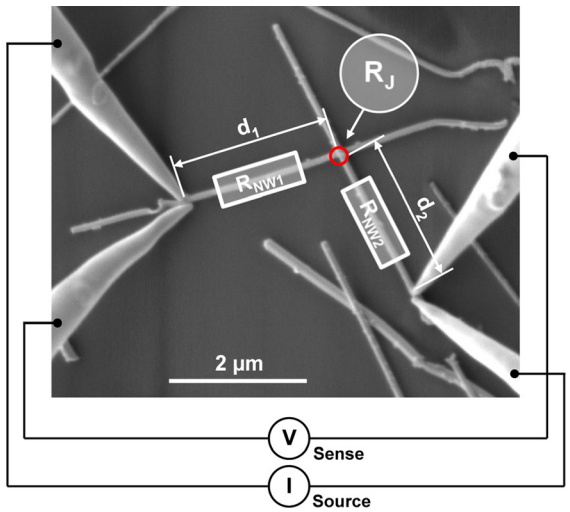

Four point probing on annealed nanowire network

Single nanowire	R_{NW}	(4.96 ± 0.18)	Ω/ µm
Junction resistance	R_J	(25.2 ± 1.9)	Ω

FIG. 1. Illustration of the used measurement setup. Nano-manipulated tungsten tips are installed inside a scanning electron microscope to contact the silver nanowires and measure the corresponding nanowire R_{NW} and junction resistances R_J by means of four point probing. Measured values on an annealed nanowire network are given in the table below.

respect to its length. By determining the total distance $d_{total} = d_1 + d_2$ between the contact positions and using the known R_{NW}, the R_J can be calculated. The analysis of our data leads to an average nanowire resistance of $R_{NW} = (4.96 \pm 0.18)\,\Omega/\mu m$. By using Pouillet's law for resistors with uniform cross-section ($R = \rho \cdot l \cdot \pi^{-1} r^{-2}$) and a resistivity of $\rho \approx 2.78 \times 10^{-8}\,\Omega m$ (for AgNWs with a diameter of 100 nm),[13] a theoretically calculated resistance for a single AgNW of our used dispersion (mean diameter of 90 nm) of about $4.40\,\Omega/\mu m$ can be obtained, which is in good accordance with the measured value of $R_{NW} = 4.96\,\Omega/\mu m$. By means of the latter value, we can extract an average nanowire junction resistance of $R_J = (25.2 \pm 1.9)\,\Omega$ for annealed AgNWs.

The annealed nanowire network is the focus of our analysis. It represents the simplest case for a mathematical description of a percolation network due to the elimination of the main disruptive factors, such as residues from the synthesis or native metal oxide. Following the spraying of AgNWs on glass, the samples are heated on a hot plate for 90 min at 210 °C. The corresponding specular transmittance values T_{spec} are plotted in dependency of their R_S (red open circles) in the diagram of Fig. 2. The curve shows the expected behavior known from literature.[14] In our direct measurement of R_{NW} and R_J, we have obtained a nanowire resistance of $R_{NW} = (4.96 \pm 0.18)\,\Omega/\mu m$ and a junction resistance of $R_J = (25.2 \pm 1.9)\,\Omega$. Accordingly, we simulated networks with a fixed $R_{NW} = 5\,\Omega/\mu m$ and various R_J values in the range of 0…250 Ω. The data obtained from the simulation are displayed in Fig. 2 as well (dashed, dotted, and dash dotted lines). By comparing the simulated data with the measurement (red open circles), a very good agreement was achieved for a junction resistance of $R_J = 30\,\Omega$ (red dashed line). Consequently, both our measurement of R_{NW} and R_J,

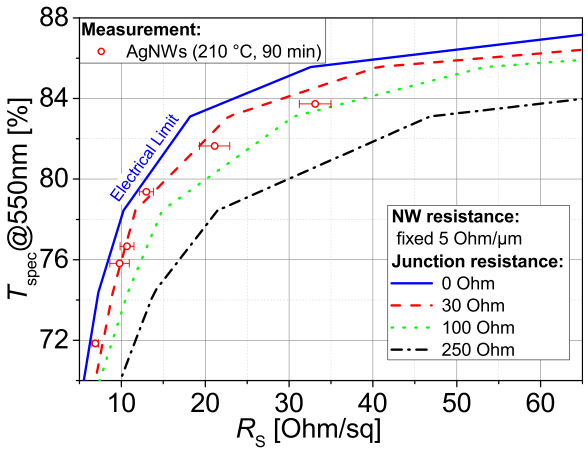

FIG. 2. Specular transmittance T_{spec} versus sheet resistance R_S of a set of annealed silver nanowire samples (210 °C, 90 min) with different transmittance values (red open circles) in comparison to simulated nanowire networks with a constant nanowire resistance $R_{NW} = 5\,\Omega/\mu$m and a variation in the junction resistances R_J (lines).

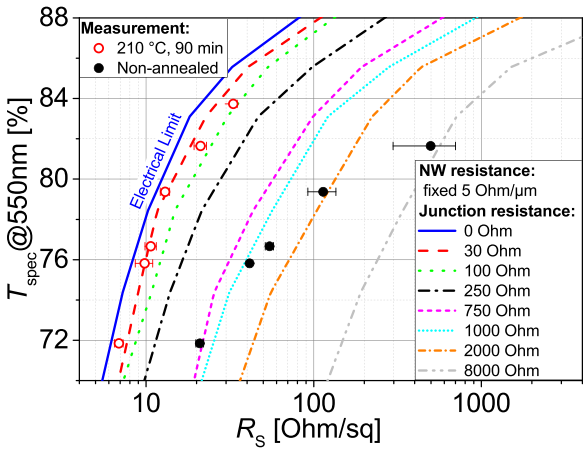

FIG. 3. Specular transmittance T_{spec} versus logarithmic sheet resistance R_S of a set of non-annealed silver nanowire samples (black circles). Subsequently, theses were annealed at 210 °C for 90 min (red open circles). The data of the samples are compared to respective simulated nanowire networks with a fixed nanowire resistance $R_{NW} = 5\,\Omega/\mu$m and a variation in the junction resistances R_J (lines).

as well as the reliability of our simulation tool is validated, enabling a meaningful estimation of the electrical limit of AgNW networks. This was carried out by extrapolating R_J to zero. Thereby, we obtain the sheet resistance limit for our used AgNW system represented by the blue solid line in Fig. 2. Comparing this curve with the measurement (red open circles), a theoretical R_S reduction by only ≈20 % would remain. In fact, the resistance at a nanowire junction will never be zero, since there are always insulating organic capping agents around metallic NWs grown in solution. Polymer residues, usually polyvinylpyrrolidone (PVP) from the synthesis, some oxidized metal, or other impurities will harm the electrical contact at the junctions. Therefore, highly conductive nanowire networks improving substantially upon the state-of-the-art cannot just be realized by reducing R_J: A possible enhancement would only be achievable by an improved nanowire geometry, meaning a higher aspect ratio (length vs. diameter) as already suggested by De *et al.*[14] Another way would be the search for new concepts, such as recently reported on bio-inspired networks.[15]

For comparison, we have also investigated the case of a non-annealed nanowire network. These networks can have substantially higher junction resistance while exhibiting a nanowire resistance of around $5\,\Omega/\mu$m (obtained from direct measurement) which is nearly identical to the resistance value in annealed nanowire electrodes. In Fig. 3, we show the corresponding results (black circles) alongside the annealed case (red open circles) and the simulated curves ($R_{NW} = 5\,\Omega/\mu$m, $R_J = 0\ldots8000\,\Omega$). All simulated curves, including the annealed data, show the same shape in this semilogarithmic plot. There is only an offset toward higher R_S values upon an increase in junction resistance. Interestingly, the non-annealed data deviate from this characteristic behavior by showing a stretched shape. Accordingly, one will not obtain a simulated curve which fits well with the data of the initial samples by progressively increasing the junction resistance. Considering the measurement with the nano-manipulator setup, an average value of $R_J = (529 \pm 239)\,\Omega$ is obtained for non-annealed wires. Here, especially the relative deviation from the mean by ±45% is comparatively large, suggesting broad distribution of junction resistance. Therefore, we investigated the influence of different R_J distributions in our simulation. We used (1) Gaussian distributions with different widths, (2) uniform distributions with various intervals, and (3) a distribution of two distinct values R_{J1} and R_{J2} with a defined ratio (e.g., $R_{J1} = 30\,\Omega : R_{J2} = 750\,\Omega$ (1:8)). Nevertheless, we still obtain curve progressions with the same shape than for the case where we input a fixed junction resistance value. The different shapes of the non-annealed and simulated curves may originate from our simple approach concerning the transmittance. In our simulation, we define the transmittance via the surface coverage, which is the percental area covered by NWs. According to Chung *et al.*,[16] we assumed that this surface coverage is equal to T_{spec}. In corresponding measurements published recently by our group,[17] we have seen a slight increase in the total transmittance of annealed AgNWs. This transmittance increase in annealed networks may originate from a closer and tighter alignment of NWs on the substrate. Therefore, we believe that the annealed system of denser arranged wires is almost identical with the ideal case of one-dimensional stick-like nanowires. Thus, this allows to directly relate the specular transmittance with the surface coverage. In addition, it is also appropriate to use the measured specular transmittance of annealed for non-annealed NWs.

In fact, we found a reasonable explanation for the deviation between measurement and simulation of the non-annealed data in our spraying procedure for complete transmittance sets. In order to obtain samples with different transmittance, one needs to spray more than just one layer of NWs on the substrate. During spraying on already deposited NWs, the ethanol in the AgNW dispersion moistens the initial NWs. At the same time, the PVP on the substrate and in the AgNW dispersion is able to connect to the shell of the NWs via hydrophobic interactions. Subsequently, as the ethanol dries, the PVP shrinks and presses the NWs toward the substrate. Thereby, better connections are established at the junctions leading to a significant reduction in sheet resistance.[18] This effect should be more pronounced for a higher

number of layers sprayed on the substrate. Especially in the region with low transmittance, a smaller difference between annealed and non-annealed networks should be visible. Considering the corresponding data in Fig. 3, one nicely observes a smaller R_S difference for low transmittance. Additionally, it should be mentioned that we heat our samples at 80 °C during spraying in order to guarantee a fast ethanol evaporation and to achieve homogeneous AgNW films. For complete transmittance sets, we usually leave the substrates on the hot plate as long as the desired T_{spec} value is reached. Therefore, especially non-annealed samples with lower transmittance are unintentionally treated somewhat longer than their counterparts with higher transmittance.

Based on the complex processes involved in the preparation of the non-annealed samples, we conclude that the corresponding data cannot be described by just one simulation curve. Most likely, every single data point represents a different network, exhibiting its own mean junction resistance which then could be fitted by our simulation tool. According to the above described influence of PVP in the sample preparation, we expect a lower mean junction resistance for samples with lower transmittance. Considering Fig. 3, one can derive a mean junction resistance of $R_J \approx 750\,\Omega$ to the network with a transmittance of 72%. At a higher transmittance of 82%, one can attribute a higher R_J of approximately $8000\,\Omega$, clearly supporting our assumption. Therefore, we are confident that a non-annealed NW network needs to be separately investigated at each transmittance value, while annealed networks show always the same mean junction resistance for each coverage.

In conclusion, we have measured the basic network parameters, including the junction resistance R_J and nanowire resistance R_{NW} of pristine and annealed AgNW networks. The resulting data allow to predict the electrical limit of our nanowire networks. From the measurement on the annealed AgNWs (210 °C, 90 min), we obtain $R_{NW} = (4.96 \pm 0.18)\,\Omega/\mu m$ and $R_J = (25.2 \pm 1.9)\,\Omega$. Putting these values into a simple model, we are able to fit the simulated curve with the data of real and optimized AgNW networks. The annealed AgNWs are quite close to the limit with a theoretical enhancement range of only 20% (common absolute $R_S \approx 10\,\Omega/sq$). Therefore, we conclude that a significant performance improvement will only be possible via a geometrical enhancement. In particular, the NW aspect ratio (length vs. diameter) needs to be increased, which means that wires with larger lengths are required. Nonetheless, very long NWs possess serious practical problems for organic solar cells. Due to the poor local contact between solar cell devices and noncontinuous NWs, low charge carrier extraction and, therefore, a low fill factor are expected. Accordingly, the incorporation of conducting interlayers or implementation of new beneficial network arrangements, e.g., bio-inspired structures, is ultimately important to maintain sufficient fill factors.

This work was funded by the European Community's Seventh Framework Program (FP7/2007-2013) under Grant Agreement No. 314068 and within the DFG Cluster of Excellence "Center for Advancing Electronics Dresden."

[1]C. F. Guo and Z. Ren, Mater. Today **18**, 143–154 (2015).
[2]F. Guo, X. Zhu, K. Forberich, J. Krantz, T. Stubhan, M. Salinas, M. Halik, S. Spallek, B. Butz, E. Spiecker, T. Ameri, N. Li, P. Kubis, D. M. Guldi, G. J. Matt, and C. J. Brabec, Adv. Eng. Mater. **3**, 1062–1067 (2013).
[3]F. Selzer, N. Weiß, D. Kneppe, L. Bormann, C. Sachse, N. Gaponik, A. Eychmüller, K. Leo, and L. Müller-Meskamp, Nanoscale **7**, 2777–2783 (2015).
[4]T. Cheng, Y. Zhang, W.-Y. Lai, and W. Huang, Adv. Mater. **27**, 3349–3376 (2015).
[5]F. C. Krebs, H. Spanggard, T. Kjr, M. Biancardo, and J. Alstrup, Mater. Sci. Eng., B **138**, 106–111 (2007).
[6]M. Niggemann, B. Zimmermann, J. Haschke, M. Glatthaar, and A. Gombert, Thin Solid Films **516**, 7181–7187 (2008).
[7]J. Lee, I. Lee, T.-S. Kim, and Y.-J. Lee, Small **9**, 2887–2894 (2013).
[8]T. Tokuno, M. Nogi, M. Karakawa, J. Jiu, T. T. Nge, Y. Aso, and K. Suganuma, Nano Res. **4**, 1215–1222 (2011).
[9]L. Hu, H. S. Kim, J.-Y. Lee, P. Peumans, and Y. Cui, ACS Nano **4**, 2955–2963 (2010).
[10]E. C. Garnett, W. Cai, J. J. Cha, F. Mahmood, S. T. Connor, M. Christoforo, Y. Cui, M. D. McGehee, and M. L. Brongersma, Nat. Mater. **11**, 241–249 (2012).
[11]D. Y. Choi, H. W. Kang, H. J. Sung, and S. S. Kim, Nanoscale **5**, 977–983 (2013).
[12]J.-Y. Lee, S. T. Connor, Y. Cui, and P. Peumans, Nano Lett. **8**, 689–692 (2008).
[13]A. Bid, A. Bora, and A. K. Raychaudhuri, Phys. Rev. B **74**, 035426 (2006).
[14]S. De, P. J. King, P. E. Lyons, U. Khan, and J. N. Coleman, ACS Nano **4**, 7064–7072 (2010).
[15]B. Han, Y. Huang, R. Li, Q. Peng, J. Luo, K. Pei, A. Herczynski, K. Kempa, Z. Ren, and J. Gao, Nature Commun. **5**, 5674 (2014).
[16]C.-H. Chung, T.-B. Song, B. Bob, R. Zhu, and Y. Yang, Nano Res. **5**, 805–814 (2012).
[17]N. Weiß, L. Müller-Meskamp, F. Selzer, L. Bormann, A. Eychmüller, K. Leo, and N. Gaponik, R. Soc. Chem. Adv. **5**, 19659–19665 (2015).
[18]F. Selzer, N. Weiß, L. Bormann, C. Sachse, N. Gaponik, L. Müller-Meskamp, A. Eychmüller, and K. Leo, Org. Electron. **15**, 3818–3824 (2014).